Broadband Spectroscopy of Nanoporous-Gold Promoter

S. Kuwano-Nakatani[1], Y. H. Han[1], T. Takahashi[2] and T. Awano[1*]

[1] Tohoku Gakuin University, Japan
[2] Research Reactor Institute, Kyoto University, Japan
*corresponding author: awano@tjcc.tohoku-gakuin.ac.jp

Abstract

The efficiency of UV photocatalysis on TiO_2 particles was increased by mixing TiO_2 particles with nanoporous gold (NPG) with pore diameters of 10–40 nm. This means that NPG acts as a promoter in the photocatalytic reaction of TiO_2. Broadband spectroscopic results from millimeter wave to ultra violet of NPG membrane are discussed to estimate plasmonic effect on the catalysis.

1. Introduction

It is well known that bulk Au is inert. However, Au nanoparticles with several-nanometer-scale sizes are catalytically active for several chemical reactions such as the decomposition of formaldehyde and oxidation of CO[1,2]. The catalytic activity depends on the size of nanoparticles. The nanoparticles with diameters in the range of 2 to 5 nm show the highest activity for oxidation[3]. Nanoporous Au (NPG) with 10–50 nm pore size also shows catalytic activity for oxidation[2].

Recently, TiO_2 is being widely used for photocatalysis of various materials. TiO_2 has a different activity with crystal structure for different wavelengths. It has been reported that composite materials of TiO_2 with Au or Pt nanoparticles enhance TiO_2 catalytic activity[4]. TiO_2 plays an active role in the decomposition of water to generate OH radicals. It is supposed that the plasmonic electromagnetic effect of Au or Pt enhances the catalytic activity of TiO_2. In addition, since pores of NPG are able to trap the TiO_2 particles on its surface, NPG seems to be a photocatalytic nanocomposite because of enhancement of the catalytic activity by the electromagnetic effect. We have found that NPG acts as a promoter to produce OH radicals using TiO_2[5]. We report optical properties of NPG in this paper to investigate electromagnetic and plasmonic origin of the promotor effect.

2. Experimental

NPG films were obtained by nitric acid etching of Ag from $Au_{35}Ag_{65}$ alloy films with about 100 nm thickness. The average pore diameter was 10–40 nm, according to the dealloying temperature and time. Figure 1 shows SEM images of NPG films with average pore diameters of 20 nm (a) and 42 nm (b). The other samples were confirmed to have average pore diameters of 11 and 33 nm.

Reflectivity spectra of the NPG films on quartz plate were measured over four regions: (1) millimeter wave region was measured using a coherent transition radiation induced by the LINAC facility of Research Reactor Institute, Kyoto University; (2) far-infrared region was measured using synchrotron radiation by UVSOR facility of Institute for Molecular Science. This region was also measured using a Martin-Puplett interferometer JASCO FARIS-1 with a
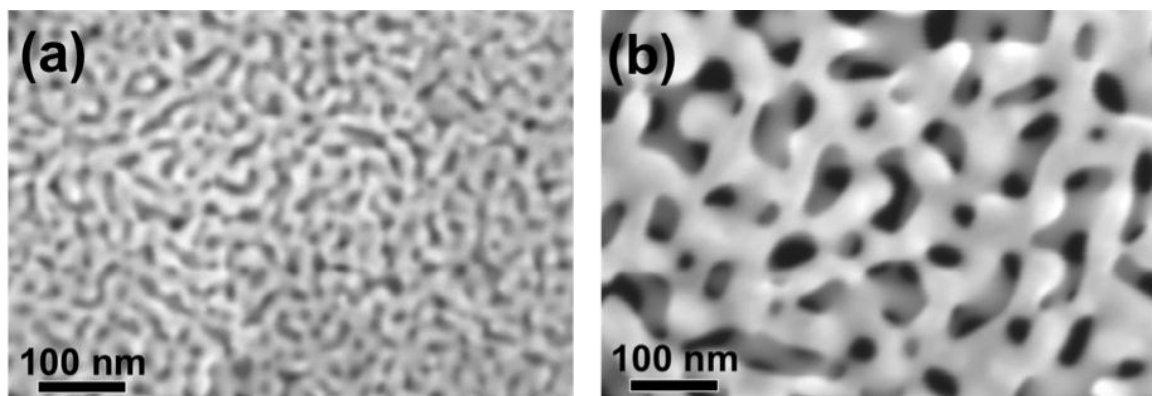

Figure 1: SEM images of NPG films. Pore diameter is (a) 20 nm and (b) 42 nm.

conventional mercury light source; (3) infrared region was measured using JASCO FT-4100 spectrometer; (4) near infrared, visible and ultraviolet region.

3. Results and discussion

3.1. Promoter effect

Anatase (25 nm average diameter) and rutile (85 nm average diameter) TiO_2 particles were in the ratio 4:1. The mixture of
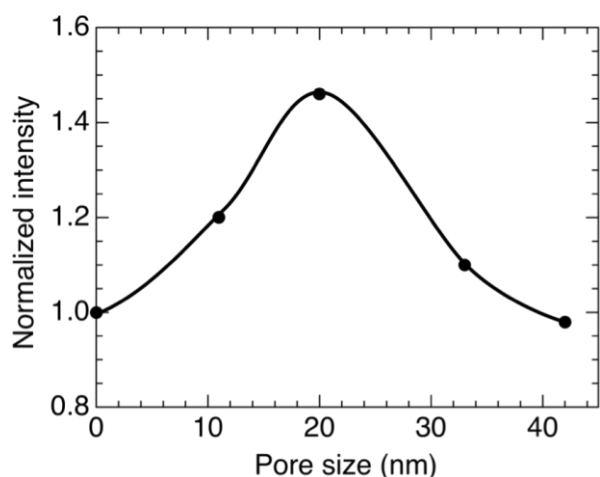

Figure 2: OH-radical production efficiency as a function of average pore diameter.

NPG, TiO_2, and spin trapping agent was irradiated by Black-light with wave length 365 nm. The spectra for the estimation of the amount of induced OH radicals were measured by X-band ESR. No OH radical was formed by the $Au_{35}Ag_{65}$ alloy film or NPG film alone during the Black-light irradiation. Besides, the coexistence of TiO_2 particles and NPG films enhanced the production of the OH radical. ESR signals of the OH-radical spin adduct were observed, and it was confirmed that NPG is a promoter for photocatalysis on TiO_2. Fig. 2 shows the efficiency of OH radical productivity vs. average pore sizes. The maximum efficiencies normalized by that of an $Au_{35}Ag_{65}$ alloy film was 1.5 at average pore diameter of 20 nm. No enhancement was observed at pore diameters over 40 nm. This peak seems to be due to that the average particle diameter of the anatase TiO_2 particles, which are sensitive to the irradiated Black-light, was 25 nm. Therefore, the active anatase TiO_2 particles appear to dispersively infiltrate into the pores of Au and tightly stick to the pore surface. This seems to enhance the promoter effect of Au on TiO_2.

3.2. Spectroscopic results

3.2.1. Reflectivity spectra

Fig. 3 shows broadband reflectivity spectra of NPG with various average pore sizes. The horizontal axis is in a logarithm to show the wide spectral range. Fine structures in IR spectra are due to CO_2 and H_2O in atmosphere. Measurement of the lack region at terahertz wave is under way at the UVSOR facility. Peaks at 0.06eV are due to reflection of the substrate quartz. It is especially strong at
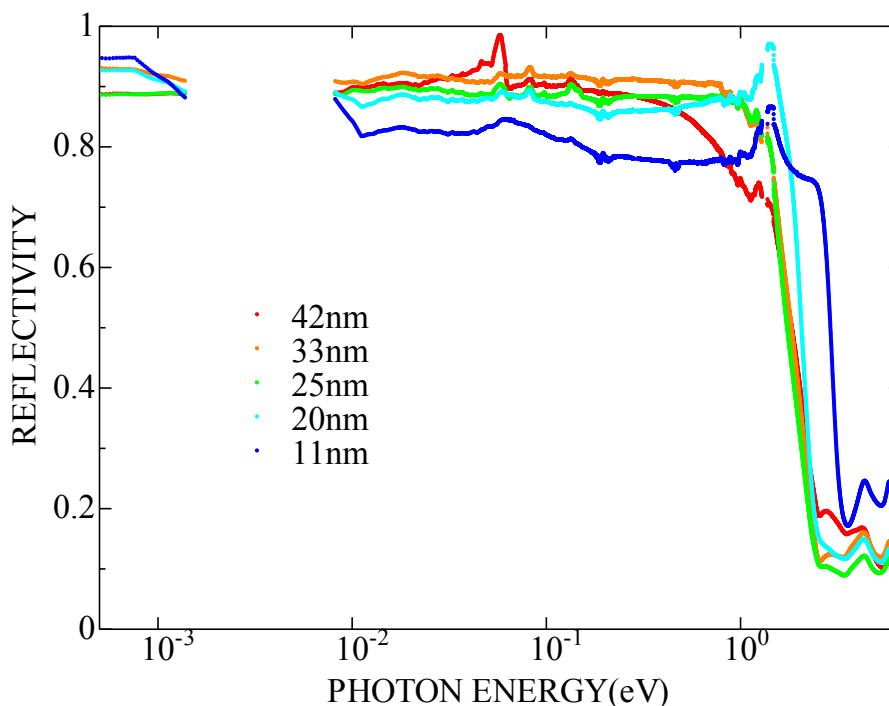

Figure 3: Reflectivity spectra of NPG membranes on quartz substrates. Average pore diameters of the five samples with diameter on the order of 42 nm to 11 nm are shown in the NIR-UV figure.
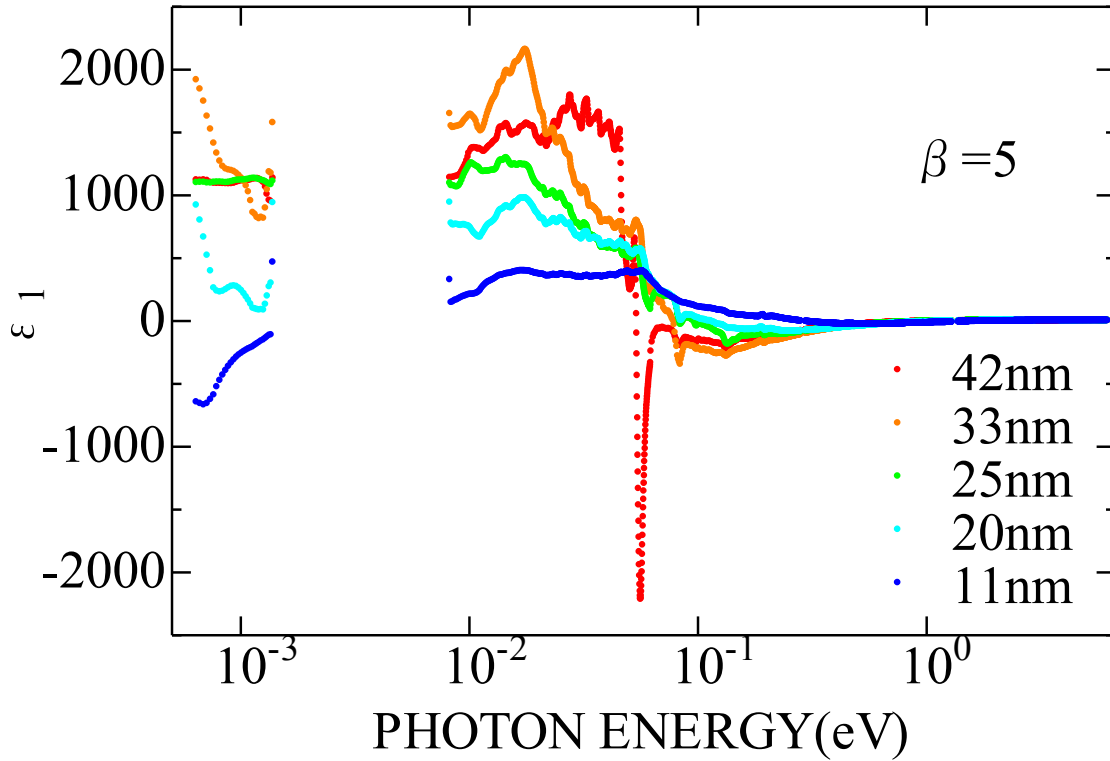
Figure 4: Dielectric constant spectra (real part) of NPG membranes on quartz substrates. The extrapolation exponent index of the reflectivity at high energy $\beta = 5$.

42nm pore sample because of void content (low average density) of the large porous thin film. Small structures at infrared region are due to absorption by CO_2 and H_2O in atmosphere. Peaks at 1.45eV are due to reflectivity dip of the reference Al mirror. Plasmonic characteristic spectral changes were observed from IR to UV region. They depend on the pore size.

3.2.2. Dielectric constants

Dielectric constants are obtained by Kramer-Kronig analysis. The measured reflectivity spectra were wide enough to obtain dielectric constants by calculation from it. The reflectivity spectra were extrapolated as constant to connect smoothly at low energy side and terahertz region. They were extrapolated as exponential decrease function to connect smoothly. The optimum exponent coefficients were scattered largely. Fig. 4 and 5 show dielectric constants at the exponent $\beta = 5$ to see the pore size dependence of optical properties. Fig. 4 shows real parts of the dielectric

constant. The large structures at 0.06eV are due to the reflection of the substrate quartz. Spectra at low energy region change as sequent by pore sizes except the case of 42nm. This seems to be due to low average density of gold by pore volume.

Fig. 5 shows imaginary parts of the dielectric constant. Lower figure shows a log-log plot to show the region from infrared to UV. The large structures at 0.06eV are due to the reflection of the substrate quartz. Spectra at low energy region change as sequent by pore sizes except the case of 42nm as in the ε_1 spectra. It is clearly observed in the lower figure that the spectra of large and intermediate pore sizes show linear decrease which means these spectra decrease as power function in the region from 0.1 to 1eV. The ε_2 spectra shows absorption intensity for transverse wave. To investigate plasmonic absorption for longitudinal wave, energy loss function spectra obtained from these dielectric constants spectra are discussed in the next section.
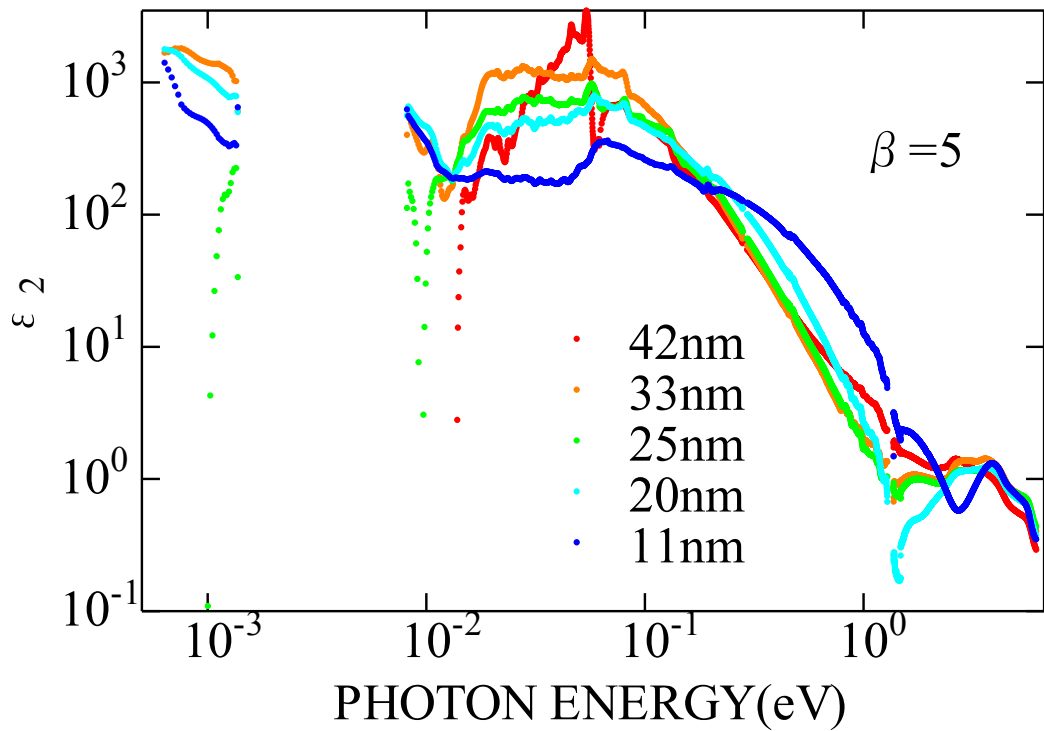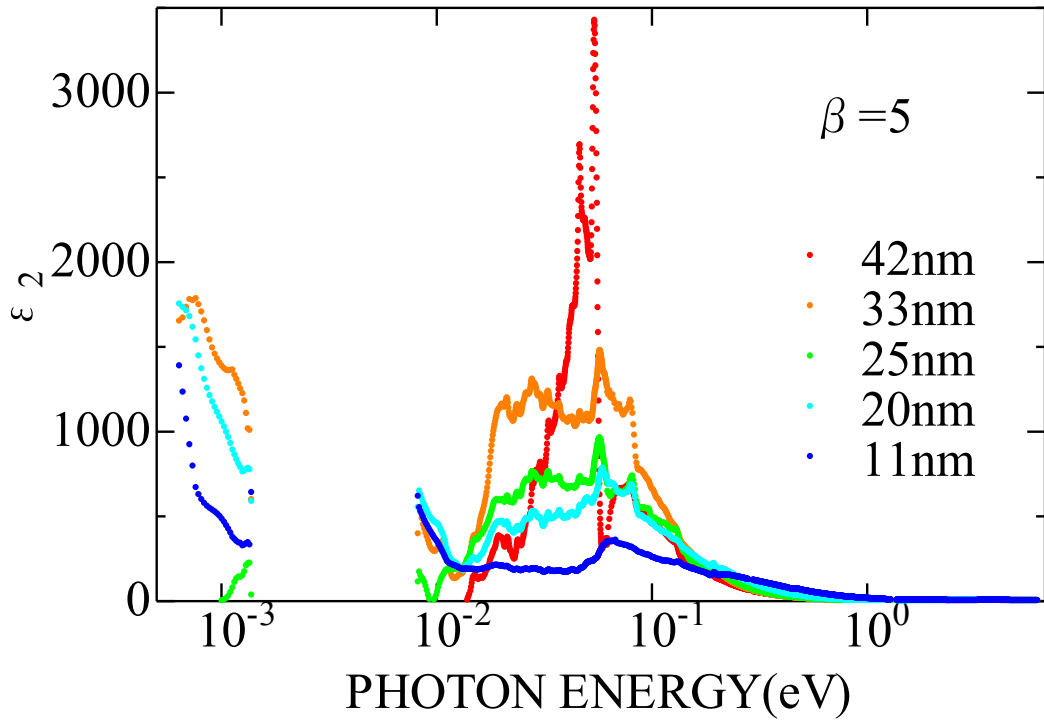
Figure 5: Dielectric constant spectra (imaginary part) of NPG membranes on quartz substrates. The above figure is semi-log plot and the below one is log-log plot. The extrapolation exponent index of the reflectivity at high energy $\beta = 5$.
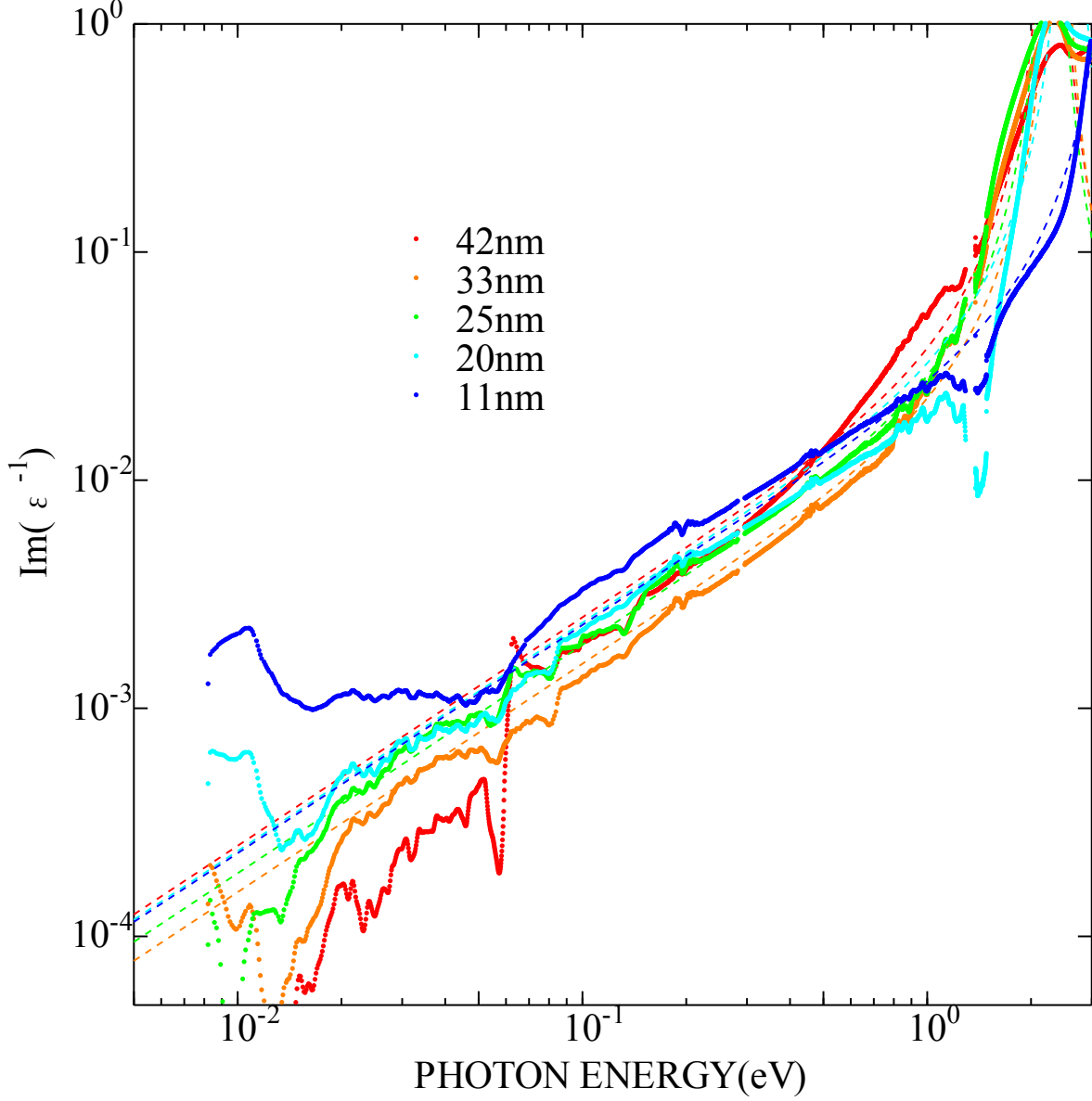
Figure 6: Drude curve fitting of the energy loss function spectra of NPG membranes on quartz substrates. Dashed lines show fitting curves for each pore size sample.

3.2.3. Plasmon fitting

Plasmon fitting by classical Drude model in energy loss function spectra is shown in fig. 6. In Drude model, dielectric constant is

$$\varepsilon = \varepsilon_\infty (1 - \frac{\omega_p^2}{\omega^2 + \gamma^2} + i\frac{\gamma\omega_p^2}{\omega(\omega^2 + \gamma^2)}),$$

where $\omega_p = \sqrt{\dfrac{4\pi N e^2}{m^* \varepsilon_\infty}}$ is the plasma frequency, γ is

dumping factor and ε_∞ is dielectric constant at high frequency. Energy loss function, $\mathrm{Im}(1/\varepsilon)$, is proportional to absorption intensity by transverse wave. The plasmon fitting

parameters are summarized in Table 1. Systematic decrease of the plasma frequency with pore size increment was observed. Plasma frequency of bulk gold is 8.6eV, therefore, these ω_p for pore samples are much small. The promoter effect seems to be related with small values of these parameters. The origin of pore size dependence of the promoter effect is still not clear.

Table 1: Plasmon parameters.

pore size(nm)	ω_p(eV)	γ (eV)	ε_∞
42	2.3	0.06	2.2
33	2.4	0.01	9
25	2.3	0.025	4
20	2.6	0.02	8
11	3.6	0.03	10

4. Conclusions

Promoter effect was discovered on NPG/TiO$_2$ system. The detail enhance mechanism of the promoter effect is not clear yet. However, we could observe that smaller plasmon parameters on NPG than those on bulk gold.

Acknowledgements

References

[1] Bierner, J. et al., Surface-chemistry-driven actuation in nanoporous gold, *Nature Materials* 8: 47–51, 2009.

[2] Wittstock, A., V. Zielasek, J. Biener, C. M. Friend, M. Bäumer, Nanoporous Gold Catalysis for Selective Gas-Phase Oxidative Coupling of Methanol at Low Temperature, *Science* 327: 319-322, 2003.

[3] Haruta, M., When Gold Is Not Noble: Catalysis by Nanoparticles, *Chem. Rec.*.3: 75-87, 2003.

[4] Haruta, M., Nanoparticulate Gold Catalysis for Low-Temperature CO Oxidation, *J. New Mat. Electrochem. Sys.* 7: 163-172, 2004.

[5] Kuwano-Nakatani S., T. Ando, K. Oba and Y.H. Han, to be published.